arXiv:2204.11479v5 [cs.SD] 5 Jul 2022

END-TO-END AUDIO STRIKES BACK: BOOSTING AUGMENTATIONS TOWARDS AN EFFICIENT AUDIO CLASSIFICATION NETWORK

Avi Gazneli, Gadi Zimerman, Tal Ridnik, Gilad Sharir, Asaf Noy
DAMO Academy, Alibaba Group
{avi.g, gadi.zimerman, tal.ridnik, gilad.sharir, asaf.noy}@alibaba-inc.com

ABSTRACT

While efficient architectures and a plethora of augmentations for end-to-end image classification tasks have been suggested and heavily investigated, state-of-the-art techniques for audio classifications still rely on numerous representations of the audio signal together with large architectures, fine-tuned from large datasets. By utilizing the inherited lightweight nature of audio and novel audio augmentations, we were able to present an efficient end-to-end (e2e) network with strong generalization ability. Experiments on a variety of sound classification sets demonstrate the effectiveness and robustness of our approach, by achieving state-of-the-art results in various settings. Public code is available at: https://github.com/Alibaba-MIIL/AudioClassification.

1 Introduction

In signal processing, sound pattern recognition plays a crucial role with a wide range of applications. Recognition can be modeled as a classification task, whether *single-label* or *multi-label*, where the algorithm outputs predictions for class labels. A typical audio signal consists of speech, music, and other environmental sounds. Environment sound refers to a wide range of classes spanning from sea waves through engines, etc. An audio signal is typically handled by converting it to a known time-frequency (T-F) representation, usually with the help of the *spectrogram* and its compressed form, known as the *mel-spectrogram*. The former is obtained by applying *Short-Time Fourier Transform* (STFT) on the waveform and taking the magnitude, while the latter requires an additional stage in which mel filter-banks are applied for squashing the frequency axis to mel bins with logarithmic spacing. However, the use of mel-spectrogram comes at the cost of having to carefully adjust the parameters for time-frequency resolution and compression rate, which might vary for different classes. By nature, sound samples for distinct classes possess different characteristics manifested mainly in duration and frequency spectrum. Hence, finding one set of parameters suitable for all is implausible. For instance, the duration of the mouse-click event lasts several milliseconds, necessitating a shorter window size, compared to the cow mooing event, which lasts a few seconds, as depicted in Fig. 2.

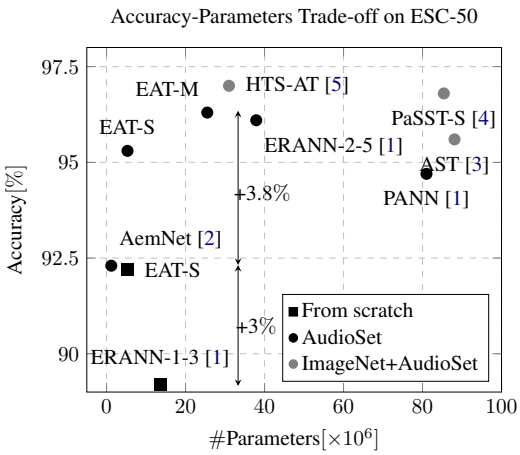

Figure 1: Comparison of our EAT architecture. Achieving SotA on 'From scratch' training (+3% from [6]) and on AudioSet pretrain (+3.8% from efficient e2e method [2])

In addition, the usage of frequency compression with logarithmic binning can also degrade the signal. For instance, chirping bird sounds naturally occupy a high-frequency band, where the transformation assigns coarsely spaced bins, as depicted in Fig. 3, which was already handled by [7, 6].

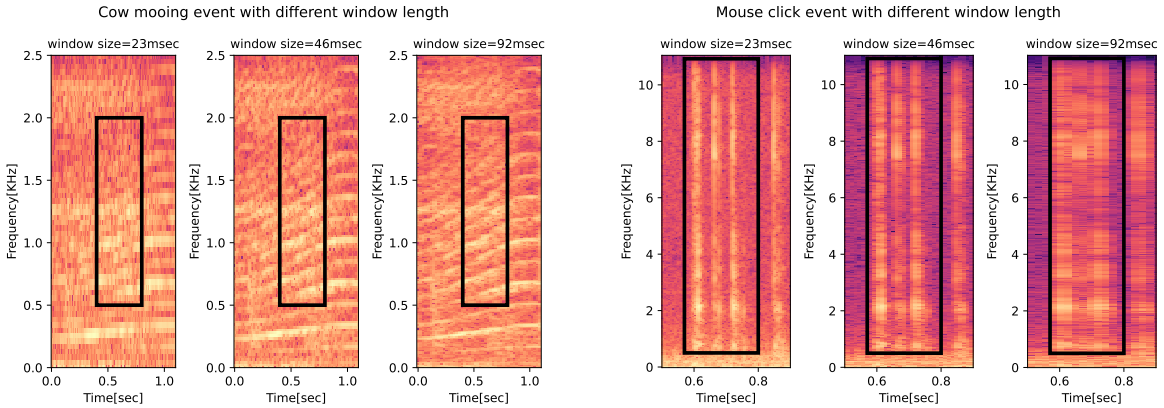

(a) (b)

Figure 2: Impact of window length on time-frequency resolution: Observing a slow event, cow mooing (a), compared to a fast event, mouse click (b) through 3 typical window lengths, with 75% overlap.

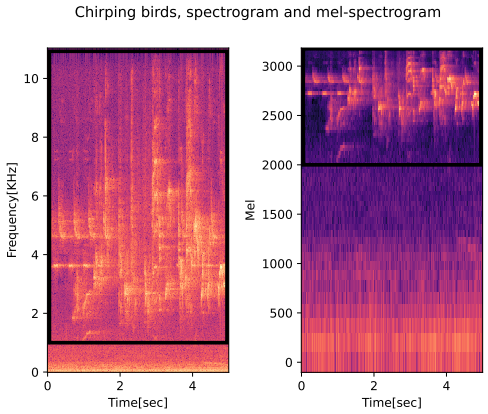

Figure 3: Impact of mel scale compression: Comparing linear frequency spacing (left) against logarithmic mel scale (right).

In audio processing, the representation issue remains an active topic. The trade-off travels from domain knowledge incorporation in signal representations at the expense of complex architectures requiring large data to fit, through end-to-end systems which maintain performance gap, mainly on limited data scenarios [8, 2, 9].
In this work we prefer the end-to-end strategy. The absence of pre-processing streamlines the system, by requiring fewer parameters to tune, and facilitates shifting between tasks with distinct signal content. Furthermore, usage of raw signal allows us to apply wide set of augmentations, including two novel schemes, which significantly decrease the gap reported in the early works. On top of data manipulation schemes, we propose a neural network, designed to handle raw audio signal characteristics. The resulted solution is simple with a low memory footprint and short inference time, as well as robust for distinct audio contents. The proposed system was evaluated on several public datasets, such as ESC-50 [10], UrbanSound8K [11], AudioSet [12] and SpeechCommands [13], achieving state of art results on several scenarios.
The contribution of the paper can be summarized as follows:

- Introducing two novel and effective augmentations for audio signals
- Designing an efficient deep learning architecture
- Demonstrating the potential of end-to-end methods, and their superiority in several audio benchmarks

2 Related Work

Audio pattern recognition systems mainly rely on transforming the raw-audio signal to time-frequency representation, mostly to a mel-spectrogram representation, and then using deep neural networks to output the class prediction. Empirically, they outperform early models which used e2e audio networks [14, 9, 7]. [15] performed a comprehensive comparison among numerous representations given the network architecture, deducing the superiority of the mel-spectrogram compared to others. The common modus operandi in deep learning is to use transfer learning from pretrained networks. [16] demonstrated the benefit of using architectures such as DenseNet [17], ResNet [18] and Inception [19] pre-trained on ImageNet [20] when applied on mel-spectrograms for the audio classification tasks. To adapt the input type to mentioned architectures, they deduced that incorporating different time-frequency resolution maps is beneficial over simple replication across the channels. The authors of [7, 21] preferred the log-spectrogram and wavelet-based representations for their ResNet50-based network. The diversity in input type may indicate on lack of robustness across tasks and require carefully adjusting the pre-defined parameters.
Several works focused on e2e architectures, albeit, there was a performance gap mainly on limited data scenarios [8, 9, 2]. Improved performance obtained by incorporating some domain knowledge with initialization [22, 21], complex architectures [1], even using additional self supervised training phase [23].
Lately, the emergence of transformers [24] infiltrated to audio processing domain with an invigorating effect. For instance, [3] applied the transformer on mel-spectrogram patches with impressive results across several datasets. In order to relax the training complexity and enabling variable size inference, [4] suggested dedicated regularization scheme during the training process together with the disentanglement of positional encoding to time and frequency axis. However, the state-of-the-art (SotA) results rely on complex models, posing hard constraints on deployment and inference.
[25] introduced a set of augmentations and became ubiquitous for spectrogram-based systems. The list involves time warping and masking the time/frequency axis. An additional widely used [26, 26, 6, 1, 3, 27] strategy is to mix pairs of samples in amplitude [9], similar to [28] on image pixels, except the mixing ratio normalized by sample gain. Our solution expands the augmentation portfolio by suggesting two novel mixing strategies, by scrambling the pairs of signals in frequency and phase, in addition to a neural network architecture dedicated to processing the signal efficiently.

3 Method

In this chapter, we describe our approach to audio classification. In general, the method involves augmenting data distribution and better integrating sound characteristics into architecture design. First, we will describe our architecture for audio classification, then we will present novel ways of augmenting sound signals.

3.1 EAT Architecture

The proposed audio classification network is shown in Fig. 4. During this stage, the primary focus was to build a neural network that has a large receptive field, while keeping complexity low. One can decompose the network into two main blocks, a 1D convolution stack, and a transformer encoder block. The former downsamples along the time axis with a convolution layer coupled to a fixed low-pass filter [29, 30], followed by intermittent residual blocks [18]. The residual blocks are modified according to [31], consisting of depth-wise convolution with a large kernel operating on the time axis, and $f(x)$ is convolution with kernel size equal to 1 operating across channels. At this point, the signal is decimated using a sequence of factors d_i by an overall factor of $d = \prod d_i$. For instance, signal with a 5-second duration the downsampling sequence is equal to $[4, 4, 4, 4]$, performing a reduction by a factor of 256. This can be to some extent linked to downsampling performed during spectrogram operation[1]. The following building blocks perform additional reduction, with each followed by a stack of dilated residual blocks [32]. This refinement enables to increase in the receptive field per frame, hence being more robust to variable duration events among the classes in environmental sound scenarios. Gathering feature maps across frames was implemented using a transformer encoder block, which followed by fully connected layer to project the embedding vector to class space. For complexity analysis and details about EAT-S and EAT-M models refer to Appendix C.

3.2 Data Augmentation

Data augmentation is a ubiquitous step during the training phase for deep learning networks, particularly in the case of limited data. [8, 9, 2] already pointed out the inferiority of e2e audio-based systems in case of limited data. This

[1] Depending on the sampling rate and STFT parameters, for example, the typical choice for 22.05KHz can be window size equal to 1024 with hopping of 256, which effectively decimates by 256 the time axis.

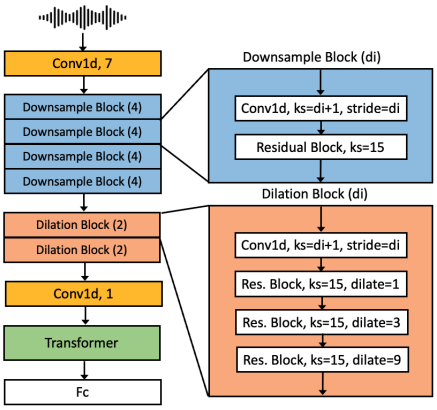

Figure 4: The proposed EAT architecture, CNN-style backbone followed by a transformer.

can be mitigated to some extent by enriching the list of augmentations. We noticed that specifically, augmentations involving label mixing were beneficial for generalization. We suggest mixing frequency bins and phases and naming them as *FreqMix* and *PhaseMix*. In FreqMix, alg. [1], given pair of samples with corresponding labels, we perform the mix by choosing low-frequency bins from one sample and concatenating with high frequency with another sample, or vice versa. The operation is equivalent to applying ideal filters in frequency domain and adding their results. In addition to the mixup [28] operation, FreqMix contributes to enlarging the size of in-between samples, by introducing a convex combination of filtered versions of the pair, Equation 1. The filtering erases a small amount of information in the frequency domain from the original sample, and fills the filtered spectrum portion from its counterpart. Sound signals are rarely narrow-band, such as a pure sine wave, thus removing a segment of contiguous frequency is unlikely to erase the entire data. The mixing, in addition spans the linear behaviour for in-between samples, to larger set than the original mixup.

$$\begin{aligned} \textbf{MixUp}&: x_{mix}[n] = \lambda \cdot x_1[n] + (1-\lambda) \cdot x_2[n] \\ \textbf{FreqMix}&: x_{mix}[n] = x_1[n] * h_1[n;\lambda] + x_2[n] * h_2[n;\lambda] \end{aligned} \tag{1}$$

where, $h_1[n;\lambda]$, $h_2[n;\lambda]$ are low-pass and high-pass filters parametrized by λ, controlling the cut-of frequency.
Raw audio maintains an additional signal characteristic, the phase. To demonstrate that phase contains some amount of discriminative information, we conducted an experiment, as described in Appendix A, in which we synthesized waveforms from the phase of the signal and trained our neural network. The classification result was significantly higher than the random guess, as detailed in Table 7. As a consequence, we suggest adding more robustness by mixing the phase among the samples, and name it PhaseMix. In PhaseMix, alg. [2], the amplitude of the original signal remains, while phase is mixed. The level of mixing is dictated according to the mixing ratio, which is randomly drawn in each iteration.
These two mixing strategies come on top of applying modified mixup [9] and cutmix [33] that we adopted for the 1D case, with results summarized in Table 6.
In addition to the transformations involving the mixing of labels, we used transforms that preserved labels, such as amplitude manipulation, re-sampling, filtering, time-shifting, and a variety of noises. It is worth mentioning that working with raw signals enables incorporating larger set of transformations with mathematical interpretations. Shifting the signal in time, for example, is reflected in the frequency domain by adding linear phase. This has no affect when working with spectrogram, where the magnitude step by definition discards phase. Furthermore, mimicking the time shift by shifting the spectrogram along the time axis, is not an equivalent operation, since time shift and absolute value are not interchangeable.
With the proposed augmentation scheme, the early reported gap for limited data scenarios [8, 9, 2] was eliminated. The whole set of transforms detailed in Table 1.

4 Experiments

In this section we will provide the experiments conducted on public classification benchmarks, such as ESC-50 [10], AudioSet [12] UrbanSound8K [11]. In addition to ESC scenarios, we examined the system on SpeechCommands [13] dataset, containing spoken words in English, to show some robustness to audio signal type. During the training process, we used AdamW [35] optimizer with maximal learning rate of $5 \cdot 10^{-4}$ and one cycle strategy [36]. In addition, we use

Algorithm 1 FreqMix

let (x_1, y_1), (x_2, y_2) be samples from dataset X
$X_1 = STFT(x_1)$,
$X_2 = STFT(x_2)$
$\lambda \sim U[0.5, 1], \quad p \sim U[0, 1]$
$k_c = int(\lambda \cdot n_{fft})$
$X_{mix} = \begin{cases} X_1[n_{fft} - k_c :, :] \oplus X_2[: k_c, :] & p \leq 0.5 \\ X_1[: k_c, :] \oplus X_2[n_{fft} - k_c :, :] & p > 0.5 \end{cases}$
$x_{mix} = ISTFT(X_{mix})$
$y_{mix} = \lambda \cdot y_1 + (1 - \lambda) \cdot y_2$

Algorithm 2 PhaseMix

let (x_1, y_1), (x_2, y_2) be samples from dataset X
$X_1 = STFT(x_1)$
$X_2 = STFT(x_2)$
$\phi_1[k, l] = \angle X_1[k, l]$
$\phi_2[k, l] = \angle X_2[k, l]$
$\lambda \sim U[0, 1]$
$\lambda_y = 0.5 \cdot \lambda + 0.5$
$\phi_{mix} = \lambda \cdot \phi_1 + (1 - \lambda) \cdot \phi_2$
$X_{mix}[k, l] = |X_1[k, l]| \cdot e^{j\phi_{mix}[k,l]}$
$x_{mix} = ISTFT(X_{mix})$
$y_{mix} = \lambda_y \cdot y_1 + (1 - \lambda_y) \cdot y_2$

weight decay with 10^{-5}, EMA [37, 38] with decay rate of 0.995 and SKD [39]. The loss is label-smoothing with a noise parameter set to 0.1 for single-label classification tasks, and binary cross-entropy for the multi-label classification case. When applying mixing augmentations we use multi-label objective and use binary cross-entropy, as suggested by [40]. To handle distinct sample lengths across datasets we adjust the parameter controlling the downsample of the network. The set of augmentations used is detailed 1, with one noise type and one mixing strategy being randomly selected in each iteration.

4.1 ESC-50

The *ESC-50* set [10] consists of 2000 samples of environmental sounds for 50 classes. Each sample has a length of 5 seconds and is sampled at 44.1KHz. The set has an official split into 5 folds. We resampled the samples to 22.05KHz for being compliant with the majority of other works, and followed the standard 5-fold cross-validation to evaluate our model. Each experiment repeated three times and averaged to final score.

Table 1: List of label preserving and label mixing augmentations

Name	Description
amplitude	random amplitude to whole or fragment of sample
noise	white, blue, pink, violet, red, uniform, phase noise
time shift	linear/cyclic with integer and fractional delay
filtering	low/high pass filter with randomized cutoff frequency
invert polarity	multiply by -1
time masking	similar to cutout [34], masking fragment of sample
quantization	quantize sample using μ law or linear regime
mixup	mixing amplitude [28], [9]
timemix	mixing in time axis, similar to cutmix [33]
freqmix	alg.[1]
phasemix	alg.[2]

Table 2: ESC-50, accuracy with model size and inference time measured on P-100 machine.

Model	e2e	Pretrained	Accuracy[%]	#Parameters[$\times 10^6$]	time[$msec$]
ESResNet-Att [7]	✗	none	83.15	32.6	11.3
ERANN-1-3 [6]	✗	none	89.2	13.6	-
EnvNet-v2 [9]	✓	none	84.9	101	2.7
AemNet WM1.0 [2]	✓	none	81.5	**5**	-
EAT-S	✓	none	**92.15**	**5.3**	8.3
PANN [1]	✗	AudioSet	94.7	81	-
ERANN-2-5 [6]	✗	AudioSet	**96.1**	37.9	-
AemNet-DW WM1.0 [2]	✓	AudioSet	92.32	**1.2**	-
EAT-S	✓	AudioSet	95.25	5.3	8.3
EAT-M	✓	AudioSet	**96.3**	25.5	9.6
AST [3]	✗	ImageNet+AudioSet	95.6	88.1	26.7
PaSST-S [4]	✗	ImageNet+AudioSet	**96.8**	85.4	25.4
HTS-AT [5]	✗	ImageNet+AudioSet	**97**	**31**	-

It is evident from the results that our method is more effective than others under the same settings. In absence of external data, the next in line in accuracy [6] possess $\times 2.6$ more parameters, while similar model size network [2] has a 10% gap in accuracy. In the AudioSet fine-tuned case, we manage achieve SotA while being 33% lighter than [6].

4.2 UrbanSound8K

UrbanSound8K is an audio dataset containing 8732 labeled sound samples, belonging to 10 class labels, split to 10 folds. The samples last up to 4 seconds and the sampling rate varies from 16KHz-48KHz. The classes are drawn from the urban sound taxonomy and all excerpts are taken from field recordings [2]. The experiment was conducted on the official 10 fold split, with samples resampled to 22.05KHz and zero-padding the short samples to 4 seconds.

Table 3: UrbanSound8K, accuracy with model size and inference time measured on P-100 machine

Model	e2e	Pretrained	Accuracy[%]	#Parameters[$\times 10^6$]	time[$msec$]
ESResnet-Att [7]	✗	none	82.76	32.6	11
AemNet WM1.0 [2]	✓	none	81.5	**5**	-
ERANN-1-4 [6]	✗	none	83.5	24.1	-
EAT-S	✓	none	**85.5**	**5.3**	8.5
ERANN-2-6 [6]	✗	AudioSet	**90.8**	54.5	-
EAT-S	✓	AudioSet	88.1	**5.3**	8.5
EAT-M	✓	AudioSet	**90**	25.5	9.6
ESResNeXt-fbsp [21]	✗	ImageNet+AudioSet	89.14	25	18.5

The results on the UrbanSound8K dataset, detailed in Table 3, follow the same pattern as on the ESC-50, Table 2, by outperforming previous approaches in the limited data scenario, while being competitive in the fine-tune mode.

4.3 SpeechCommands

Speech Commands V2 [13] is a dataset consisting of $\sim 106K$ recordings for 35 words with a 1-second duration, with a sampling rate equal to 16KHz. The set has an official train, validation, and test split with $\sim 84K$, $\sim 10K$, and $\sim 11K$ samples, respectively. Our experiment involves the 35-class classification task.

In Table 4, we see that our approach achieves SotA results even without using external data, while being at least $\times 6$ lighter than other methods. Furthermore, demonstrating that our method is robust to additional content, such as speech.

[2] Can be found at `www.freesound.org`

Table 4: Speech Commands V2 (35 classes), accuracy with model size and inference time measured on P-100 machine

Model	e2e	Pretrained type	Result[%]	#Parameters[$\times 10^6$]	time[$msec$]
AST [3]	✗	ImageNet	98.11	87.3	11
HTS-AT [5]	✗	AudioSet	98.0	31.0	-
EAT-S	✓	none	**98.15**	**5.3**	7.5

4.4 AudioSet

AudioSet [12] is a collection of over 2 million 10-second audio clips excised from YouTube videos with a class ontology of 527 labels covering a wide range of everyday sounds, from human and animal sounds, to natural and environmental sounds, to musical and miscellaneous sounds. The set consist of two subsets, named *balanced* with $20K$ samples and *unbalanced* training with $2M$ samples, with evaluation set with $20K$ samples. The noise augmentations were excluded during training due to the presence of noise, and pink noise in class labels.

Table 5: Audioset, mAP with model size and inference time measured on P-100, w/o external data

Model	e2e	Pretrained	mAP[%]	#Parameters[$\times 10^6$]	time[$msec$]
AST [3]	✗	none	36.6	88.1	63.5
ERANN-1-6 [6]	✗	none	**45.6**	54.5	14[3]
AemNet WM1.0 [2]	✓	none	33.16	**5**	-
HTS-AT [5]	✗	none	**45.3**	31	-
EAT-S	✓	none	40.5	**5.3**	8.4
EAT-M	✓	none	42.6	25.5	14.6

Table 5, evidently demonstrates the advantage of training a large model, for fitting large sets. Yet, our method can be a considered a good balance in terms of accuracy vs efficiency, without apparent affect on downstream tasks.

4.5 Efficiency and edge deployment

In this section the focus will be on model complexity. Complexity translates to model size and inference time, which can induce costs and inflexibility for platforms and applications. Our EAT-S model has 5.3M parameters, which resembles the proportion of MobileNet-V2 architecture [41] in both size and inference time, as detailed in Appendix B. This makes EAT-S a candidate for deploying audio classification capabilities in low-memory edge devices.

4.6 Ablation study

In this section we explore the impact of our suggestions for augmentations and architecture. The experiments were conducted on the ESC-50 dataset.

Table 6: Ablations - Classification results conducted on ESC-50 (incremental improvements over baselines)

(a) Baseline 83% (without any mix)

Model	Relative accuracy to baseline[%]
+mixup	+3.5
+cutmix	+0.5
+freqmix	+3.1
+phasemix	+0.9

(b) Baseline 80.5% (without architecture modification)

Block	Relative accuracy to baseline[%]
+modified residual blocks	+1.8
+dilated residual blocks	+6.5
+transformer	+2

For Tables 6a and 6b , in each experiment, we incrementally add to the baseline and report the relative result. For the augmentation ablation study, Table 6a, the baseline refers to not applying any mixing augmentations, while in the architecture ablation study, Table 6b, the baseline refers to our architecture without the suggested modifications - (a)

[3] Measured on V-100 machine [6]

modified residual block and dilated residual blocks vs. common residual block and (b) transformer vs. convolution layer with global average pooling. We can see from Tables 6a and 6b that in both cases, the increments significantly improve the accuracy.

5 Conclusions

In this paper, we presented new audio augmentations and a novel, simple and efficient architecture for sound classification. We were able to show, through analysis and experiments, that end-to-end audio systems can no longer be considered inferior, especially in low data scenarios. The suggested scheme achieves state of the art results in several datasets both in 'from-scratch' and AudioSet-pretraining setups, all while being exceptionally light-weight and robust. Future work can elaborate this work to solve additional tasks and contents, such as sound event detection, localization or speech and speaker recognition.

References

[1] Qiuqiang Kong, Yin Cao, Turab Iqbal, Yuxuan Wang, Wenwu Wang, and Mark D Plumbley. Panns: Large-scale pretrained audio neural networks for audio pattern recognition. *IEEE/ACM Transactions on Audio, Speech, and Language Processing*, 28:2880–2894, 2020.

[2] Paulo Lopez-Meyer, Juan A del Hoyo Ontiveros, Hong Lu, and Georg Stemmer. Efficient end-to-end audio embeddings generation for audio classification on target applications. In *ICASSP 2021-2021 IEEE International Conference on Acoustics, Speech and Signal Processing (ICASSP)*, pages 601–605. IEEE, 2021.

[3] Yuan Gong, Yu-An Chung, and James Glass. Ast: Audio spectrogram transformer. *arXiv preprint arXiv:2104.01778*, 2021.

[4] Khaled Koutini, Jan Schlüter, Hamid Eghbal-zadeh, and Gerhard Widmer. Efficient training of audio transformers with patchout. *arXiv preprint arXiv:2110.05069*, 2021.

[5] Ke Chen, Xingjian Du, Bilei Zhu, Zejun Ma, Taylor Berg-Kirkpatrick, and Shlomo Dubnov. Hts-at: A hierarchical token-semantic audio transformer for sound classification and detection. *arXiv preprint arXiv:2202.00874*, 2022.

[6] Sergey Verbitskiy, Vladimir Berikov, and Viacheslav Vyshegorodtsev. Eranns: Efficient residual audio neural networks for audio pattern recognition. *arXiv preprint arXiv:2106.01621*, 2021.

[7] Andrey Guzhov, Federico Raue, Jörn Hees, and Andreas Dengel. Esresnet: Environmental sound classification based on visual domain models. In *2020 25th International Conference on Pattern Recognition (ICPR)*, pages 4933–4940. IEEE, 2021.

[8] Jordi Pons, Oriol Nieto, Matthew Prockup, Erik Schmidt, Andreas Ehmann, and Xavier Serra. End-to-end learning for music audio tagging at scale. *arXiv preprint arXiv:1711.02520*, 2017.

[9] Yuji Tokozume, Yoshitaka Ushiku, and Tatsuya Harada. Learning from between-class examples for deep sound recognition. *arXiv preprint arXiv:1711.10282*, (1), 2017.

[10] Karol J Piczak. Esc: Dataset for environmental sound classification. In *Proceedings of the 23rd ACM international conference on Multimedia*, pages 1015–1018, 2015.

[11] Justin Salamon, Christopher Jacoby, and Juan Pablo Bello. A dataset and taxonomy for urban sound research. In *Proceedings of the 22nd ACM international conference on Multimedia*, pages 1041–1044, 2014.

[12] Jort F Gemmeke, Daniel PW Ellis, Dylan Freedman, Aren Jansen, Wade Lawrence, R Channing Moore, Manoj Plakal, and Marvin Ritter. Audio set: An ontology and human-labeled dataset for audio events. In *2017 IEEE International Conference on Acoustics, Speech and Signal Processing (ICASSP)*, pages 776–780. IEEE, 2017.

[13] Pete Warden. Speech commands: A dataset for limited-vocabulary speech recognition. *arXiv preprint arXiv:1804.03209*, 2018.

[14] Jongpil Lee, Jiyoung Park, Keunhyoung Luke Kim, and Juhan Nam. Sample-level deep convolutional neural networks for music auto-tagging using raw waveforms. *arXiv preprint arXiv:1703.01789*, 2017.

[15] Muhammad Huzaifah. Comparison of time-frequency representations for environmental sound classification using convolutional neural networks. *arXiv preprint arXiv:1706.07156*, 2017.

[16] Kamalesh Palanisamy, Dipika Singhania, and Angela Yao. Rethinking cnn models for audio classification. *arXiv preprint arXiv:2007.11154*, 2020.

[17] Forrest Iandola, Matt Moskewicz, Sergey Karayev, Ross Girshick, Trevor Darrell, and Kurt Keutzer. Densenet: Implementing efficient convnet descriptor pyramids. *arXiv preprint arXiv:1404.1869*, 2014.

[18] Kaiming He, Xiangyu Zhang, Shaoqing Ren, and Jian Sun. Deep residual learning for image recognition. In *Proceedings of the IEEE conference on computer vision and pattern recognition*, pages 770–778, 2016.

[19] Christian Szegedy, Wei Liu, Yangqing Jia, Pierre Sermanet, Scott Reed, Dragomir Anguelov, Dumitru Erhan, Vincent Vanhoucke, and Andrew Rabinovich. Going deeper with convolutions. In *Proceedings of the IEEE conference on computer vision and pattern recognition*, pages 1–9, 2015.

[20] Jia Deng, Wei Dong, Richard Socher, Li-Jia Li, Kai Li, and Li Fei-Fei. Imagenet: A large-scale hierarchical image database. In *2009 IEEE conference on computer vision and pattern recognition*, pages 248–255. Ieee, 2009.

[21] Andrey Guzhov, Federico Raue, Jörn Hees, and Andreas Dengel. Esresne(x)t-fbsp: Learning robust time-frequency transformation of audio, 2021.

[22] Tycho Max Sylvester Tax, Jose Luis Diez Antich, Hendrik Purwins, and Lars Maaløe. Utilizing domain knowledge in end-to-end audio processing. *arXiv preprint arXiv:1712.00254*, 2017.

[23] Luyu Wang and Aaron van den Oord. Multi-format contrastive learning of audio representations. *arXiv preprint arXiv:2103.06508*, 2021.

[24] Niki Parmar, Ashish Vaswani, Jakob Uszkoreit, Lukasz Kaiser, Noam Shazeer, Alexander Ku, and Dustin Tran. Image transformer. In *International Conference on Machine Learning*, pages 4055–4064. PMLR, 2018.

[25] Daniel S Park, William Chan, Yu Zhang, Chung-Cheng Chiu, Barret Zoph, Ekin D Cubuk, and Quoc V Le. Specaugment: A simple data augmentation method for automatic speech recognition. *arXiv preprint arXiv:1904.08779*, 2019.

[26] Hendrik Purwins, Bo Li, Tuomas Virtanen, Jan Schlüter, Shuo-Yiin Chang, and Tara Sainath. Deep learning for audio signal processing. *IEEE Journal of Selected Topics in Signal Processing*, 13(2):206–219, 2019.

[27] Yuan Gong, Yu-An Chung, and James Glass. Psla: Improving audio tagging with pretraining, sampling, labeling, and aggregation. *IEEE/ACM Transactions on Audio, Speech, and Language Processing*, 29:3292–3306, 2021.

[28] Hongyi Zhang, Moustapha Cisse, Yann N Dauphin, and David Lopez-Paz. mixup: Beyond empirical risk minimization. *arXiv preprint arXiv:1710.09412*, 2017.

[29] Richard Zhang. Making convolutional networks shift-invariant again. In *International conference on machine learning*, pages 7324–7334. PMLR, 2019.

[30] Tal Ridnik, Hussam Lawen, Asaf Noy, Emanuel Ben Baruch, Gilad Sharir, and Itamar Friedman. Tresnet: High performance gpu-dedicated architecture. In *Proceedings of the IEEE/CVF Winter Conference on Applications of Computer Vision*, pages 1400–1409, 2021.

[31] Jaeseong You, Gyuhyeon Nam, Dalhyun Kim, and Gyeongsu Chae. Axial residual networks for cyclegan-based voice conversion. *arXiv preprint arXiv:2102.08075*, 2021.

[32] Kundan Kumar, Rithesh Kumar, Thibault de Boissiere, Lucas Gestin, Wei Zhen Teoh, Jose Sotelo, Alexandre de Brébisson, Yoshua Bengio, and Aaron C Courville. Melgan: Generative adversarial networks for conditional waveform synthesis. *Advances in neural information processing systems*, 32, 2019.

[33] Sangdoo Yun, Dongyoon Han, Seong Joon Oh, Sanghyuk Chun, Junsuk Choe, and Youngjoon Yoo. Cutmix: Regularization strategy to train strong classifiers with localizable features. In *Proceedings of the IEEE/CVF International Conference on Computer Vision*, pages 6023–6032, 2019.

[34] Terrance DeVries and Graham W Taylor. Improved regularization of convolutional neural networks with cutout. *arXiv preprint arXiv:1708.04552*, 2017.

[35] Ilya Loshchilov and Frank Hutter. Decoupled weight decay regularization. *arXiv preprint arXiv:1711.05101*, 2017.

[36] Leslie N Smith. A disciplined approach to neural network hyper-parameters: Part 1–learning rate, batch size, momentum, and weight decay. *arXiv preprint arXiv:1803.09820*, 2018.

[37] Antti Tarvainen and Harri Valpola. Mean teachers are better role models: Weight-averaged consistency targets improve semi-supervised deep learning results. *Advances in neural information processing systems*, 30, 2017.

[38] Pavel Izmailov, Dmitrii Podoprikhin, Timur Garipov, Dmitry Vetrov, and Andrew Gordon Wilson. Averaging weights leads to wider optima and better generalization. *arXiv preprint arXiv:1803.05407*, 2018.

[39] Linfeng Zhang, Jiebo Song, Anni Gao, Jingwei Chen, Chenglong Bao, and Kaisheng Ma. Be your own teacher: Improve the performance of convolutional neural networks via self distillation. In *Proceedings of the IEEE/CVF International Conference on Computer Vision*, pages 3713–3722, 2019.

[40] Ross Wightman, Hugo Touvron, and Hervé Jégou. Resnet strikes back: An improved training procedure in timm. *arXiv preprint arXiv:2110.00476*, 2021.

[41] Mark Sandler, Andrew Howard, Menglong Zhu, Andrey Zhmoginov, and Liang-Chieh Chen. Mobilenetv2: Inverted residuals and linear bottlenecks. In *Proceedings of the IEEE conference on computer vision and pattern recognition*, pages 4510–4520, 2018.

Appendices

A Phase waveform synthesis

We assumed that the audio signal's phase component may contain discriminative information. To confirm this assumption, we synthesized waveforms from the phase of the signal. Spectrogram based representations inherently ignore the phase, by taking only the magnitude. Mathematically this is equivalent to filtering the original signal with a unit amplitude filter with the opposite phase, as described at equations [2, 3]:

$$\begin{aligned} X[k,l] &= STFT\left(x[n]\right) \\ X[k,l] &= |X[k,l]| \cdot e^{j\phi[k,l]} \\ |X[k,l]| &= X[k,l] \cdot e^{-j\phi[k,l]} \end{aligned} \tag{2}$$

Which can rephrased as filtering operation -

$$\begin{aligned} |X[k,l]| &= X[k,l] \cdot H[k,l] \\ h[n] &= ISTFT(H[k,l]) \end{aligned} \tag{3}$$

The "phase" waveform was extracted according to equation 3. For this experiment, the classifier was trained (a) on the original signal, (b) signals based on phase, (c) signals based on the magnitude, and (d) on both (b)+(c), concatenated to produce a 2-dimensional input signal. The experiment was conducted on the ESC-50 dataset, with noise and mixing augmentations being disabled [4].

Table 7: ESC-50, accuracy vs input content

Mode	Accuracy[%]
phase	60
magnitude	78.5
phase+magnitude	80.5
baseline	81

From Table 7 we can see two outcomes. At first, the phase signal resulted in significantly higher accuracy than a random guess. Second, seems that this information is complementary to the magnitude signal. These observations lead us to augment the phase domain during the training process, by adding phase noise and mixing the phases among pairs of signals.

B Inference time details

Table 8 details the inference time for various network configurations.

Table 8: Inference time measured on V-100 machine, and Intel(R) Xeon(R) CPU E5-2682 v4 @ 2.50GHz on EAT-S model

sample length[s]	gpu-time[ms]	cpu-time[ms]
1	5.3	38.3
5	5.5	67
10	5.6	145

[4] Due to the noisy nature of the phase signal

C EAT Models - Architectures details

Table 9 details the configuration for our models, EAT-S/M. "Channels" refers to number of filter at the first stage of the network.

Table 9: Architecture details

Model	Channels	Transformer layers/heads	embedding dimension	#Parameters$[\times 10^6]$
EAT-S(mall)	16	4/8	128	5.3
EAT-M(edium)	32	6/16	256	25.5